UNIVERSITY of CALIFORNIA
SANTA CRUZ

NEURON STIMULATION AND APPLICATIONS TO RESTORING SIGHT THROUGH RETINAL PROTHESES

A thesis submitted in partial satisfaction of the
requirements for the degree of

BACHELOR OF SCIENCE

in

PHYSICS

by

Spencer Pequegnat

10 June 2020

Abstract

Neuron Stimulation and Applications to Restoring Sight Through Retinal Protheses

by

Spencer Pequegnat

Stimulating neurons has seen various applications in the past. The Hodgkin-Huxley electric model of neurons is summarized to understand the generation of action potentials, an important factor for neuron communication. When a portion of the neurons degenerate in the retina, the remaining neurons can be electrically stimulated. Retinal prostheses have emerged as a way to restore sight to patients blind due to loss of photoreceptors from retinal degenerations. Epiretinal and subretinal stimulation is discussed and how different layers of the retina responds to electrical stimulation. Various retinal implants are explored followed by an outlook for future hardware and software advancements of retinal implants.

Contents

List of Figures

1

Introduction

One of the earliest written record of electrical phenomena is seen in ancient Egyptian hieroglyphs dated 4000 B.C., that describe the electric sheatfish (Malmivuo et al., 1995). In the eighteenth century a connection was made between electricity and the neural system from the work of Luigi Galvani, where he observed that a frog's skeletal muscles can be contracted from dissimilar metals, attached to the frog's leg and connected together (Galvani, 1791). The simultaneous understanding of electromagnetism and neurobiology in the 19th century paved way for the development of potential applications towards areas such as medicine. Today, collaborations from multiple disciplines, including biology, physics, neuroscience, medicine, and engineering, has led to improvements in medical diagnoses and therapeutics, through electronic devices. Some of these devices include electrocardiography, imaging machines, and pacemakers. Perhaps the most remarkable are devices enabling the restoration to our senses through electrical stimulation to parts of the central nervous system.

The central nervous system consists of the brain and spinal cord and is responsible

for integrating information and communication. The brain, is a complex organ which takes in information and processes it to not only construct our everyday experiences and the ability to think, but also the ability to communicate with other parts of the body such as muscles, through neurons. However, there are many neurodegenerative diseases that inhibit the way the brain processes and communicates this information such as multiple sclerosis, where nerve damage disrupts communication between the brain and the body; Huntington's disease, an inherited condition in which nerve cells in the brain break down over time; Parkinson's, a disorder of the central nervous system that affects movement, often including tremors and through natural aging processes that lead to degradation, such as blindness. The leading cause of incurable blindness in the developed world today is a broad category of diseases known as retinal degenerations (Smith et al., 2001; Haim, 2002). Electrical stimulation is important to restore function since it bridges the gap of communication that can occur. By stimulating surviving neurons, functionality to the degenerative areas could be restored.

The success of sensory restoration through neuroprosthetics can be seen already with cochlear implants successfully restoring hearing to the deaf, functioning well enough to enable speech recognition (Eshraghi et al., 2012). Due to this success, it has inspired scientists and clinicians to try restoring vision in patients with retinal degenerations by electrical stimulation of the neurons that relay visual signals to the brain. Over the past decade, retinal prostheses have emerged as a promising technology for restoring vision loss due to retinal degeneration (Palanker & Goetz, 2018). Part of restoring vision loss is to restore visual acuity, which quantifies spatial resolution, where 20/20 is considered normal. Visual acuity is explained further in section 3.3, including the exact meaning of the number.

For retinal prostheses to be the most useful, the goal is to restore visual acuity to at least the legal blindness status of 20/200.

In the following chapter, there will be a discussion of how neurons communicate with one another through action potentials. Chapter 3 will explore how neurons are stimulated electrically, look at electronic approaches to restoring sight through neural prostheses and look forward to improvements that can be made. The final chapter will be a summary and conclusion.

2

The Neuron

2.1 Neuron Structure

The 100 billion neurons in the brain are different from most cells in the body in that they have with distinct regions, each with specific purposes. The nerve cell can be divided into three main regions: the cell body called the soma, dendrites, and the axon (Fig. 2.1). The soma, like other cell bodies, contain the nucleus and other organelles, necessary for cellular function. Dendrites are the region where one neuron receives connections from other neurons. The axon is long nerve fiber where information is transmitted from one part of the neuron to the terminal regions of the neuron. The end of the axon contains the synapse region and is where one neuron forms connections with another via chemical messengers, known as neurotransmitters.

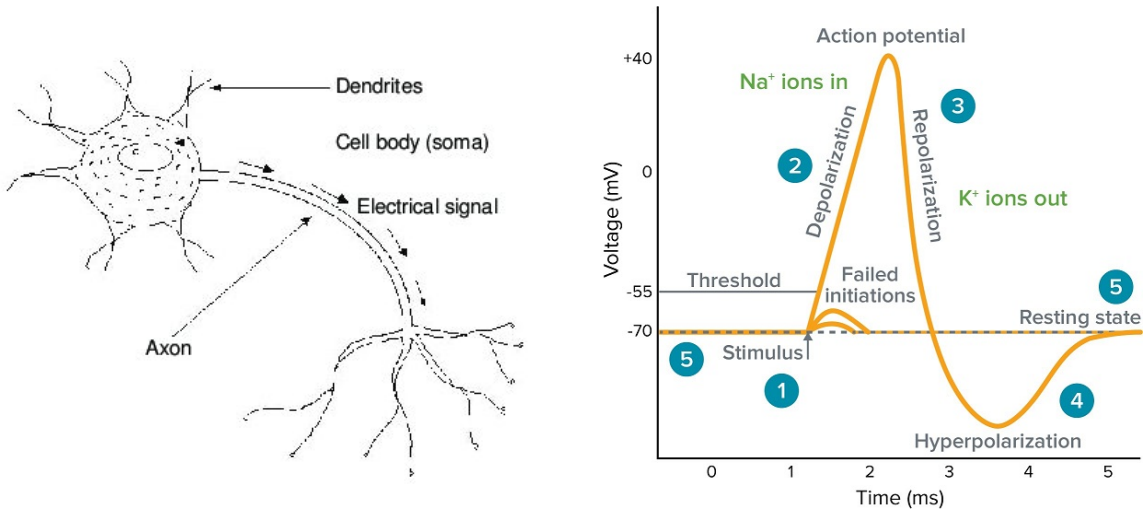

Figure 2.1: Left: A typical textbook illustration of a neuron and its regions (cell body, dendrites and axon) Right: Action potential graph showing the change in potential of the cell interior relative to outside. Major points include; 1 is the point where stimulus is introduced, 2 when depolarization occurs from the flood of Na ions into the membrane, 3 repolarization from potassium ions leaving, 4 the point of hyperpolarization, becoming more polarized than initially,and 5 returns to resting state. Failed initiations can be seen when the voltage does not exceed the threshold potential. Figures from London & Segev (2001).

2.2 The Resting and Action Potential

Inside the cell, the resting potential ranges from -80mV to -40mV, while outside the cell has zero potential. When the potential inside increases from some stimulus and exceeds the threshold potential, an action potential is generated. The action potential is associated with a rapid depolarization to achieve a peak value of about +40mV . The peak is followed by an equally rapid repolarization phase. Chemically, an action potential begins with a rush of sodium ions into the cell through sodium channels, resulting in depolarization, while recovery involves an outward rush of potassium through potassium channels (Fig 2.1 Right). An important feature of action potentials is that a larger stimulus intensity results in more action potentials and a greater frequency at which they occur. Therefore the

information is not encoded in the shape or amplitude of the action potential, but with the frequency.

2.2.1 Origin of the Resting Potential: Ionic Mechanisms

The membrane is important in establishing the electric properties of a cell through the regulation of ions flowing into or out of the cell. The inside and outside of the cell differ in ionic compositions, resulting in a diffusion gradient, with ions flowing from high to low concentrations. This flow leads to an accumulation of ions at the inner and outer membrane surfaces, resulting in an electric field established within the membrane. Describing this ion movement involves electrical field forces and diffusional forces, where an equilibrium is attained when these forces are balanced for all permeable ions. For a membrane permeable to only one ion, the equilibrium voltage is given by the Nernst equation. An extension to the Nernst equation is the Goldman-Hodgkin-Katz equation which takes into account a membrane permeable to multiple ions.

The equilibrium voltage V_k across the membrane for the k^{th} ion is given by the Nernst equation (Malmivuo et al., 1995)

$$V_k = -\frac{RT}{z_k F} ln \frac{C_{i,k}}{C_{o,k}}, \tag{2.1}$$

where R is the gas constant, T the absolute temperature in Kelvins, z_k the valence of the k^{th} ion, F the Faraday's constant, $C_{i,k}$ the intracellular concentration of the k^{th} ion, and $C_{o,k}$ the extracellular concentration of the k^{th} ion.

However since membranes are permeable not only a single ion, we must take into account several permeable ions such as sodium, potassium, and chloride. When equilibrium is reached, every ion is at it's Nernst potential, which is the common transmembrane

potential. The required equilibrium concentrations ratio must satisfy the following,

$$\frac{C_{o,K}}{C_{i,K}} = \frac{C_{o,Na}}{C_{i,Na}} = \frac{C_{i,Cl}}{C_{o,Cl}}, \tag{2.2}$$

where K, Na, and Cl represents potassium, sodium, and chlorine ions respectively. The condition in equation 2.2 where all ions are in equilibrium is known as the Donnan equilibrium (Malmivuo et al., 1995). Taking into account the relationship between membrane voltages and ionic fluxes, the potential difference V_m across the membrane is the following (Malmivuo et al., 1995):

$$V_m = -\frac{RT}{F} ln \frac{P_K C_{i,K} + P_{Na} C_{i,Na} + P_{Cl} C_{o,Cl}}{P_K C_{o,K} + P_{Na} C_{o,Na} + P_{Cl} C_{i,Cl}} \tag{2.3}$$

where P_K, P_{Na}, and P_{Cl} are the permeability of potassium, sodium, and chlorine ions respectively. Equation 2.3 is known as the Goldman-Hodgkin-Katz equation. From equation 2.3 one can see that the relative contribution of each ion to the resting voltage is weighted by the ion's permeability.

When a stimulus current pulse depolarizes the resting membrane of a cell beyond the threshold, an action potential is produced. The next section looks at a quantitative model of the action potential from the work of Hodgkin and Huxley.

2.3 Hodgkin-Huxley Membrane Model

The initiation and propagation of an action potential in a neuron was described mathematically, by Hodgkin and Huxley in 1952, where they performed a series of electrophysiological experiments on squid giant axons (Hodgkin & Huxley, 1952). They demonstrated how the ionic currents in the axon could be understood from changes in sodium and potassium conductance (reciprocal of resistance) in the axon membrane.

The model is based on the thought of a simple circuit with resistors, capacitors, and batteries. An example of this circuit can be seen in Figure 2.2. A current can be carried through the circuit as ions passing through the membrane (resistors) or by charging the capacitors of the membrane (Hodgkin & Huxley, 1952).

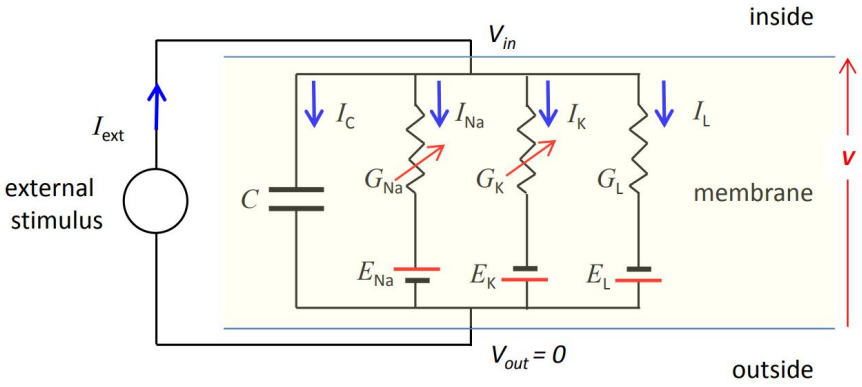

Figure 2.2: Model of the cell and its flow of current in a RC circuit diagram. Equivalently used by Hodgkin and Huxley to model the squid axon. The external stimulus I_{ext} flows through the membrane, where the currents can be represented by the current charging a capacitor I_c, the currents carried by the sodium and potassium ions, I_{Na} and I_K, and a leakage current I_l. Inside the membrane, G represents the ionic conductances (reciprocal of resistance) and E the equilibrium potentials. Figure from Cooper (2015).

The first step in their model is to divide the total membrane current into an ionic current and a capacitve current:

$$I_{ext} = C_m \frac{dV_m}{dt} + I_{ion} \tag{2.4}$$

where I_{ext} is the externally applied current or the total membrane current density, C_m is the membrane capacitance, V_m is the membrane potential V_{in} - V_{out}, and I_{ion} is the net ionic current flowing across the membrane (Hodgkin & Huxley, 1952). The reason for an equation of this form is to determine the membrane capacitance in a way that is independent of the magnitude or sign of V_m and minimally affected by the time course of V_m (Hodgkin

& Huxley, 1952).

The ionic current, I_{ion}, can be split into three components: current carried by sodium ions (I_{Na}), potassium ions (I_K), and other ions (I_L), also known as the leakage current.

$$I_{ion} = I_{Na} + I_K + I_L \tag{2.5}$$

The ionic permeability of the membrane can be expressed in terms of the ionic conductances (G_{Na}, G_K, G_L), where the individual ionic currents are given from the following relations (based on Ohm's law)

$$I_{Na} = G_{Na}(V_m - E_{Na}), \tag{2.6}$$

$$I_K = G_K(V_m - E_K), \tag{2.7}$$

$$I_L = G_L(V_m - E_L). \tag{2.8}$$

E_{Na} and E_K are the equilibrium potentials for the sodium and potassium ions, defined by the Nernst equation. E_L is the potential at which the leakage current due to chloride or other ions is zero (Hodgkin & Huxley, 1952).

Substituting equations 2.4 - 2.7 into equation 2.3 yields the total current density across the membrane

$$I_{ext} = C_m\frac{dV_m}{dt} + G_{Na}(V_m - E_{Na}) + G_K(V_m - E_K) + G_L(V_m - E_L). \tag{2.9}$$

Their experiments suggest that the sodium and potassium conductance, G_{Na} and G_K, are functions of time and membrane potential but G_L is a constant $\bar{g}_L$ (Hodgkin & Huxley, 1952). They say that "there is little hope of calculating the time course of the sodium and potassium conductances from first principles" (Hodgkin & Huxley, 1952), so their objective was to find equations for G_{Na} and G_K through experimental means, to

reasonable accuracy (Hodgkin & Huxley, 1952). From their experimental results, they determined the the equations to describe the potassium conductance:

$$G_K = \bar{g}_K n^4, \tag{2.10}$$

$$\frac{dn}{dt} = \alpha_n(1-n) - \beta_n n, \tag{2.11}$$

where $\bar{g}_K$ is a constant, α_n and β_n are rate constants which only vary with voltage and n a dimensionless variable which can vary between 0 and 1 (Hodgkin & Huxley, 1952). Physically, n is the proportion of ion channels that are open due to the rate of closing of the channels α_n, and the rate of opening β_n. Along the same lines, they determined the equations to describe the sodium conductance as:

$$G_{Na} = m^3 h \bar{g}_{Na}, \tag{2.12}$$

$$\frac{dm}{dt} = \alpha_m(1-m) - \beta_m m, \tag{2.13}$$

$$\frac{dh}{dt} = \alpha_h(1-h) - \beta_h h, \tag{2.14}$$

where $\bar{g}_{Na}$ is a constant, the α's and β's are functions of voltage, and m and h varying between 0 and 1 (Hodgkin & Huxley, 1952). Physically, m represents the proportion of activating molecules on the inside, and h is the proportion of inactivating molecules on the outside due to the transfer rates from α's and β's (Hodgkin & Huxley, 1952).

Combining equations 2.8, 2.9, 2.11 and using the fact that $G_L = \bar{g}_L$, we obtain:

$$I_{ext} = C_m \frac{dV_m}{dt} + m^3 h \bar{g}_{Na}(V_m - E_{Na}) + \bar{g}_K n^4 (V_m - E_K) + \bar{g}_L(V_m - E_L) \tag{2.15}$$

A solution to equation 2.14 can be seen in Figure 2.3, where the calculated action potential has approximately the correct form and duration.

Now with an understanding of how action potentials are generated in neurons, the next section will focus the visual information processing in the eye, specifically the retina.

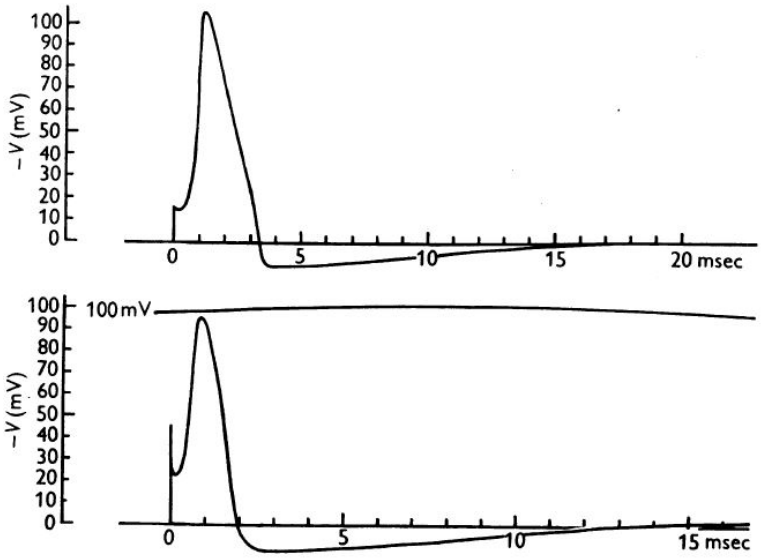

Figure 2.3: Top curve: solution to equation 2.14 with initial depolarization of 15 mV at 6 degrees Celsius. Lower curve: tracing of membrane action potential at 9.1 degree Celcius for axon 14. Figure taken from Hodgkin & Huxley (1952).

3

The Eye and Retinal Prostheses

3.1 Anatomy of the Eye

Eyes are organs of the visual system that provide the ability to receive and process visual data, through the detection of light (Figure 3.1a). The eye is a fluid-filled sphere enclosed by three layers of tissue. The outer layer is made of a tough white fibrous tissue, the sclera. At the front of the eye, it is transformed into a transparent tissue that permits light to enter the eye, called the cornea. The middle layer of tissue contains the iris, the ciliary body, and the choroid. The iris is the colored portion of the eye and is responsible for controlling the diameter and size of the pupil (the opening in its center), and thus controlling the amount of light that enters the eye. The ciliary body includes a muscular component that controls the shape of the lens, and a component that produces the fluid for the front of the eye. The choroid is the vascular layer, supplying blood to the eye, specifically the retina. The retina is the innermost layer of the eye and contains neurons which are sensitive to light and are capable of transmitting visual signals (Purves et al., 2001).

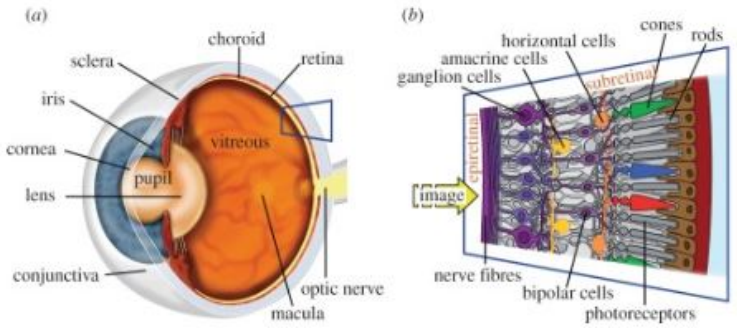

Figure 3.1: (a) The structure of the eye where vision begins with incident light coming through the cornea and lens. The light is projected onto the retina, converting the incident photons into action potentials, which in turn relays visual information via the optic nerve, to be processed by the brain. (b) The three retinal layers can be seen here. The photoreceptor layer, the inner nuclear layer, consisting of horizontal, bipolar, and amacrine cells, and the ganglion cell layer. Figure from Stingl et al. (2013a)

3.2 Visual Processing in the Retina

When incoming light travels through the cornea and lens, it is projected onto the tissue covering the back of the eye, called the retina. The light-sensitive portion of the central nervous system has three layers: the photoreceptor layer, the inner nuclear layer and the ganglion cell layer (Figure 3.1b).

Photoreceptors are neurons that do not generate action potentials. They instead convert photon energy into changes in their membrane potential via light-sensitive proteins called opsins. The photoreceptors are in contact with the retinal pigment epithelium (RPE), keeping the health and function of the photoreceptors, through the RPE cells regenerating photopigments and digesting outer segments shed by the photoreceptors.

The human retina contains about 120 million photoreceptors, made up of cones, dominating the central regions of the visual field, responsible for day vision, and rods dominating the periphery, responsible for night vision. The three types of cones include S,

M, and L (short, medium, and long wavelength), with each type more receptive to different parts of the visible light spectrum (Wandell et al., 1995).

The photoreceptors relay the gathered visual information to the other neurons in the inner nuclear layer of the retina. The neural signals move from bipolar cells to ganglion cells. Horizontal and amacrine cells perform intermediate and lateral processing at bipolar and ganglion cells, respectively. The ganglion cells generate action potentials that are relayed to the brain via axons, making up the optic nerve.

Photoreceptors are an important part of the visual processing chain. Without them there is no light being converted to membrane potential, no information is relayed to other retinal and no action potentials are generated in ganglion cells to be relayed to the brain for processes. Diseases that lose this function is explained next.

3.3 Blindness and Retinal Degeneration

The main cause of permanent blindness in developed nations is caused by a category of diseases known as retinal degenerations (Smith et al., 2001; Haim, 2002). The loss of vision comes from the progression of dying photoreceptors, but the neurons in the inner layer and ganglion cells mostly survive. This survival creates an opportunity for retinal prostheses to electrically stimulate what remains. If successful, the stimulation is carried through the optic nerve, fooling the brain into thinking you can see and create visual percepts.

For older patients, a disease known as age-related macular degeneration (AMD) usually takes place, after 60 years of age. The number of people affected worldwide by AMD is projected to be 196 million by 2020 and rising to 288 million by 2040 (Wong et al., 2014).

Throughout the progression of AMD, there is an accumulation of a yellow debris deposits called drusen, onto the macula, between the RPE layer and choroid. Drusen build up is thought to damage the retina by impeding nutrient flow from the choroid. Since Amyloid beta is a protein that builds up in AMD, similar to Alzheimer's, AMD is sometimes called "dementia of the eye" (Ratnayaka et al., 2015).

The two forms of this disease are called dry AMD and wet AMD. In the dry form, photoreceptors die from the deterioration of RPE cells in the center of the visual field. This geographic atrophy leads to a central blind spot. Wet AMD is when new blood vessels start growing from the choroid into the retina, which also degrades central vision. Drugs can help prevent this neovascularization, but they have a short lifetime in the body, and must be delivered via injection into the eye, on a monthly basis. Since AMD affects photoreceptors in the central region, the peripheral vision is somewhat intact. This enables patients to move well without a walking cane or guide dog, but have problems performing actions requiring high visual acuity, such as reading and face recognition.

Another disease that leads to loss of photoreceptors is retinitis pigmentosa, which affects 1 in 4,000 people in their twenties or thirties (Smith et al., 2001). As this inherited disease progresses photoreceptors are lost from the periphery torwards the center, leading to patients to suffer from tunnel vision.

An important characteristic of visual function is visual acuity, which is a measure of spatial resolution. Both AMD and retinitis pigmentosa lead to significant loss in visual acuity. Having a visual acuity of 20/x means that you must be as close as 20 feet to see what a person with normal vision can see at x feet. Normal vision is having an visual acuity of 20/20. Having a visual acuity of less than 20/200 means the person is considered legally

blind.

Retinal degenerations leave surviving cells in the inner nuclear layer and the ganglion cell layer, despite near total loss of photoreceptors (Humayun et al., 1999). In the later stages of these disease, changes in retinal organization occurs, know as retinal remodeling (Marc et al., 2003; Marc & Jones, 2003). Amacrine and bipolar cells move away from the center of the retina or to the ganglion cell layer, creating new circuits that are most likely damaging (Marc & Jones, 2003). These changes impact retinal signal processing and may constrain prosthetics for restoration, suggesting that neuronal organization may be more plastic than previously thought (Marc & Jones, 2003). Retinitis pigmentosa patients are more likely to suffer from remodeling than AMD patients.

3.4 Types of Retinal prosthetics

There are three categories of retinal implants, depending on it's location: epiretinal, subretinal, or supracordial (Figure 3.2).

Epiretinal prostheses target the retinal ganglion cells by placing electrodes on top of the inner limiting membrane (Humayun et al., 2012; Stingl et al., 2013b). Stimulating RGCs directly bypasses the inner nuclear layer. Epiretinal prostheses are implanted and explanted more easily than other types.

Subretinal protheses replace the degenerated photoreceptors between the inner nuclear layer and the pigment epithelium, with arrays of electrodes, that mainly target the remaining bipolar cells (Stingl et al., 2013b). These implants send visual information to non-spiking inner retinal neurons, which are converted into action potentials in the ganglion cells. A subretinal device being implanted and explanted comes with its complications.

Implantation envolves retinal detachment and reattachment, resulting in complex surgical procedures. Explanting a subretinal device is more difficult than an epiretinal one.

Suprachoroidal implants are placed between the the choroid and sclera. Due to it's location, this approach is associated with safety benefits compared to epiretinal and subretinal implants (Morimoto et al., 2011; Ayton et al., 2014). The amount of spatial resolution that can be obtained is greatly restricted due to the large distance between the electrodes and retinal neurons. The implants are placed in the periphery of the visual field, helping low-resolution vision.

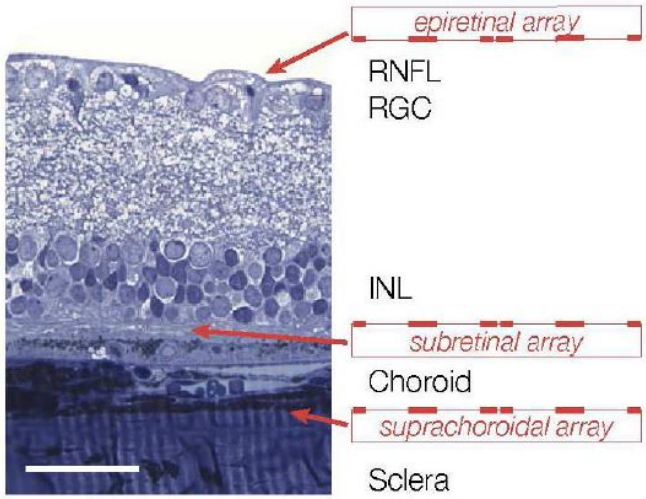

Figure 3.2: Figure of a degenerate rat retina, showing different implant placements. The epiretinal implants are in contact with the ganglion cell layer (RGC) and the subretinal array is placed in contact with the inner nuclear layer (INL) near the photoreceptors. The suprachoridal array is placed on the other side of the choroid, above the sclera. Figure image from Goetz & Palanker (2016).

3.5 Delivery of information and power

Implants transfer information and power wirelessly through one of following techniques: optical delivery of data and power, optical data transmission with power delivered through inductive coils, or delivery of power and data through inductive coils.

In medical devices power and data in transmitted via an AC current driven through an external transmitting coil inducing an AC current in the implanted receiving coil, which is then converted into DC current in the implant. A tuned resonance with frequency f is created from a capacitor in series with the receiving coil which amplifies the received voltage by Q, a quality factor. High Q coil is efficient for receiving power, but not data, and therefore separate coils are used for each (Wang et al., 2005). The Shannon-Hartley theorem (Liu et al., 2000) expresses the data capacity C of a coil as

$$C = \frac{f}{Q} log(1 + SNR), \tag{3.1}$$

with SNR being the signal-to-noise ratio of the signal.

The maximum number of pixels N that can be driven at refresh rate R with S stimulation (gray) levels is:

$$N = \frac{C}{R log_2 S}. \tag{3.2}$$

The choice of log base 2 means that the units of the information measured is in bits (binary digits). This result comes from information theory.

Retinal devices that use coils for power and data transmission include the Argus II epiretinal prothesis and has been approved by the FDA for use (Section 3.8).

Another approach is devices that transmit visual information through the natural optics of the eye and deliver only power through inductive coils (Loudin et al., 2007). The

Alpha IMS implant is one of the most well known device of this kind, where the subretinal implant is a camera with an electrode in each pixel converting incident photos into electrical stimulation. The power receiving coil is placed behind the ear and routed to the implant via a cable. This cable makes implantation difficult and can lead to problems.

The last approach to retinal implants receives both data and power directly from light, via natural optics of the eyes (Mathieson et al., 2012; Ghezzi et al., 2013). Incident light is converted into electric current to stimulate neurons. Current concepts of photovoltaic subretinal implants involve video goggles powering the implant from light projected onto them, implemented in 2007 (Loudin et al., 2007). A convenient way to process images before displaying them onto the implant is through a pocket computer. An important feature is that these photovoltaic systems do not require any wires (Mathieson et al., 2012).

3.6 Safety

There are many safety concerns when devices are implanted into the eye. An implant exposed to bodily fluids can wear away and lead to failure. If not properly encapsulated, they can cause tissue damage. This damage takes the form of a significant fibrotic or gilal seal around the device, causing an increased distance between electrodes to target cells, where close proximity is desired (Butterwick et al., 2009). Electronics in most neural implants are therefore enclosed in metallic or ceramic containers.

Tissue heating occurs from absorption of electromagnetic radiation and energy dissipation in the implanted electronic. The heating must be within safety limits, within the natural range of body temperature variation. The following equation (Sramek et al.,

2009) governs the heating induced by the implant:

$$\rho c_p \frac{\partial T}{\partial t} = \nabla(k\nabla T) + Q(x,t) - A_p(x)\rho_b c_b(T - T_0) \tag{3.3}$$

where ρ and c_p are the density and heat capacity of the medium, k is the thermal conductivity, Q is the volumetric heat source, A_p is the local blood perfusion rate, ρ_b and c_b are the density and heat capacity of the blood, and T_0 is the arterial temperature.

There is a possibility of irreversible cell damage from prolonged exposure to electrical stimulation of neural tissue (McCreery et al., 1990), including the creation of pores in the cell.

3.7 Stimulating different retinal layers

Intracellular activation of neurons can be seen from the Hodkin-Huxley equations in section 2.3. Since intracellular activation requires chronic access to the interior of the cell and direct injection of current, it lacks clinical application.

The strength-duration relationship for intracellular stimulation is most commonly cited as the Lapicque equation (Brunel & van Rossum, 2007),

$$I_{th} = \frac{I_{rh}}{1 - 2^{-\frac{\tau}{\tau_{ch}}}} \tag{3.4}$$

and the Weiss equation [34],

$$I_{th} = I_{rh}(1 + \frac{\tau_{ch}}{\tau}), \tag{3.5}$$

where I_{th} is the minimum current injected into the cell over a duration τ, I_{rh} is the rheobase current, and τ_{ch} the chronaxie time. The rheobase is the constant level of current at long durations. The chronaxie is a measure of responsiveness of a neuron and it is the time is the minimum time required for an electric current to double the strength of the rheobase.

All clinical neural implants work through extracellular electrical stimulation by polarizing cells in an electric field. Polarization of the cell occurs due to the nature of the cell membrane being very resistive and the cytoplasm inside being very conductive and therefore, when an electric field is applied, charges redistribute, creating a trans-membrane potential increase on one side and decrease on the other. As seen in earlier sections, changes in the trans-membrane potential affect the conductivity of voltage sensitive ion gates, resulting in cellular depolarization as a whole. Once the potentials pass the threshold, an action potential occurs.

The threshold current does not depend on the electrical pulse duration if an action potential occurs during the stimulation pulse. This is the rheobase region of stimulation. A shorter pulse requires a stronger stimulus in order to open up enough ion channels to exceed the stimulation threshold. This governs the rising part of the strength duration dependence of the threshold stimulation (Boinagrov et al., 2010) with decreasing pulse duration.

The chronaxie in ganglion cells is shorter than in bipolar cells. This is important for stimulating various cell types selectively. RGC responses to electrical stimulation has three categories. Short latency responses, less than 2ms, correspond to action potentials generated directly in the ganglion cells. Medium Latency responses, 3-50 ms, are stimulation of the inner nuclear layer. Long Latency responses, greater than 50 ms, are from electrical stimulation of photoreceptors. These categories highlight the ability to to selectively stimulate different retinal layers without affecting others. Selectivity is quantitatively defined as the inverse ratio of the stimulation thresholds of the target layer vs other layers.

Different retinal protheses have different selectivitys. The goal of epiretinal prostheses is to generate RGC responses through direct stimulation, therefore, selectivity for

this approach is the threshold for medium latency action potentials divided by the threshold for short latency action potentials. Epiretinal stimulation is shown to have the lowest threshold for direct RGC response and highest selectivity, over a factor of 3, with short pulses below 0.5 ms (Boinagrov et al., 2014). Subretinal protheses mainly target cells in the inner nuclear layer so the selectivity is the ratio of short latency action potentials thresholds over medium latency action potentials, with long pulses, over 4 ms, had the best selectivity, exceeding 5 for 20 ms pulses(Boinagrov et al., 2014).

Since epiretinal and subretinal implants stimulate different layers, the ganglion cell layer and inner nuclear layer respectively, the response to stimulation differs and strategies for encoding information vary. Visual information is encoded in retinal ganglion cells through action potentials and therefore epiretinal implants try to directly elicit this response through a stimulation pulse for each spike. Responses of RGCs to direct activation with electrodes have been studied (Humayun et al., 1994; Suzuki et al., 2004; Sekirnjak et al., 2006). RGCs respond to direct activation with a single action potential generated within 3 ms of the stimulation pulse, and the stronger the stimulus the greater the decrease in latency of response (Boinagrov et al., 2014). The probability of eliciting such an action potential increases with stimulus amplitude (Fried et al., 2009). Studies stimulating the area of high-density sodium channels in RGCs correspond to the region of minimum threshold for direct activation (Fried et al., 2009). Small electrodes can achieve high spatial resolution because the low required currents activate single ganglion cells, and have optimal pulse durations not exceeding the approximate range of 100-400 μs (Sekirnjak et al., 2006). However epiretinal activation of RGCs can have unintended stimulation of nearby axons, hindering focused activation of RGCs (Weitz et al., 2015). Activating axons of distant RGCs distorts

the visual information for blind patients and is a major problems for epiretinal implants. A proposed solution to unwanted axonal activation involved longer stimulation pulses greater than 25 ms, aiming to activate the inner nuclear layer instead (Weitz et al., 2015), but this approach has yet to be seen as a practical solution.

Subretinal implants aim to create activity in RGCs by stimulation of the inner nuclear layer. By not directly stimulating the RGCs and instead creating activity in the retinal network, some features of natural retinal signal processing can be kept. The processes of the retinal response to subretinal stimulation are not as well understood as from directly activating RGCs in epiretinal stimulation. The activation of bipolar cells are responsible for the action potentials from network stimulation (Freeman & Fried, 2011). The number of spikes increased with stronger and longer stimuli (Tsai et al., 2009) making it possible to control the strength of retinal response by changing pulse duration and amplitude.

3.8 Clincal results of various prosthetic devices

Prosthetic vision success is ultimately measured through some form of visual perception being restored in patients. A number of prosthetic devices have elicited meaningful visual information and therefore are confirmation that implants work for patients suffering from retinal degenerations. This chapter looks at various prothetic devices.

The Argus II is an epiretinal implant and the only approved retinal prothesis for commercial use by the FDA. The system is a three part device consisting of camera mounted glasses and processing unit that transmits data wirelessly to the implant on the retina (Figure 3.3). It contains an array of 60 stimulating electrodes attached to the epiretinal surface (Humayun et al., 2012). The 6 x 10 array of round platinum-coated electrodes are 200 μm

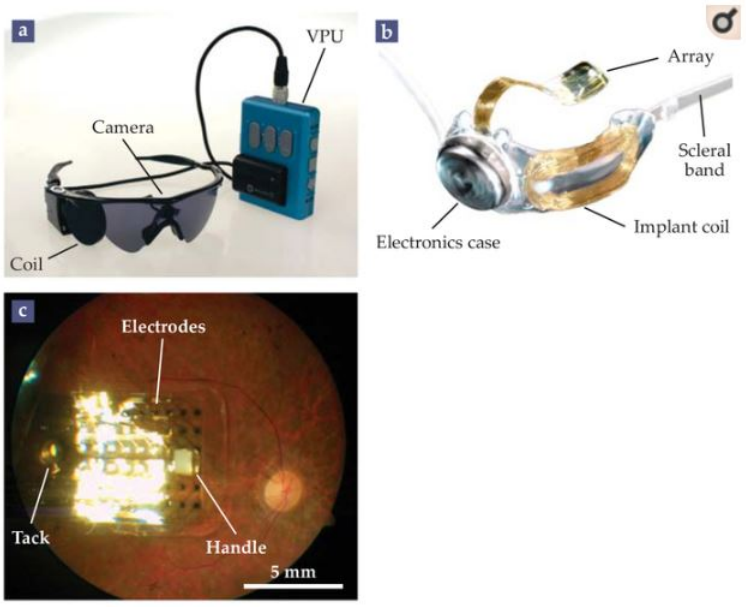

Figure 3.3: The Argus II :(a) The external components of the Argus II include glasses with a mounted camera, a visual processing unit (VPU) that converts the camera's images into AC signals, and the RF coil that transmits the signals to the implant. (b) The epiretinal implant, planted on the outside of the eye where the signal is processed and then transmitted to the array. (c) The retina with an implanted array. Figure from Palanker & Goetz (2018).

in diameter with center-to-center spacing of around 575 μm (Stronks & Dagnelie, 2014). A number of patients with a diagnosis of retinitis pigmentosa or outer retinal degeneration and with bare or no light perception in both eyes, have had the Argus II implanted with success of some visual acuity restoration (Ho et al., 2015; da Cruz et al., 2013). In a clinical trial, seventy percent of the patients did not have any serious adverse affects and those who did had conjunctival erosion or dehiscence over the extraocular implant and was treated successfully (Humayun et al., 2012). All subjects in the Argus II clinical trial were able to perceive light when turned on with a best recorded visual acuity of 20/1260 (Humayun et al., 2012). Known limitations of the Argus II result from the stimulation of axons passing between the stimulating electrodes and ganglion cells. As discussed in an earlier section, a proposed solution is to have longer pulses, 20 ms instead of 0.5 ms to stimulate bipolar

cells rather than ganglion cells, creating a network retinal responses with unwanted axonal activation, but has yet to be shown (Weitz et al., 2015).

The Alpha IMS subretinal implant has been led in Germany by Retinal Rimplant AG (Stingl et al., 2013a; Zrenner et al., 2011; Ghezzi et al., 2013). The device consists of a light sensitive photodiode-array positioned in the layer of the degenerated photoreceptors (subretinally) and stimulates the bipolar cells layer and thereby uses the processing power of the neuronal network of the inner retina (Stingl et al., 2015). The implant consists of 1500 72x72 μm^2 pixels made up of a 30x15 μm^2 photodiode and a 50x50 μm^2 Titanium Nitride electrode. (Stingl et al., 2015). Power is delivered through a cable to a receiver behind the ear like in cochlear implants (Figure 3.4). Patients included in the study has loss of vision caused by retinitis pigmentosa or other hereditary degenerations. The Alpha IMS implant positioned in the subfoveolar subretinal space has been shown to restore visual percepts in daily life for at least two-thirds of the patients investigated in a study (Stingl et al., 2013a). When the implant was placed subfoveally, all of patients could perceive light and determine light localization, seventy five percent could resolve motion, and eighty-eight percent could correctly distinguished stripe patterns (Stingl et al., 2013b). One patient had a best Landolt C-ring visual acuity of 50/550, whereas the rest of the patients had equivalent visual acuities below 20/1000 (Stingl et al., 2013a). None of the participants achieved an acuity approaching the theoretical limit of resolution of the pixel array, around 20/280. This could be from an electrode arrangement resulting in strong cross-talk between neighboring electrodes and thus may limit spatial contrast (Loudin et al., 2007). The Alpha IMS prosthesis is underperforming by a factor of 2 with respect to its sampling limit, leading some to conclude that continued reduction in pixel size will not improve visual acuity (Flores

et al., 2019).

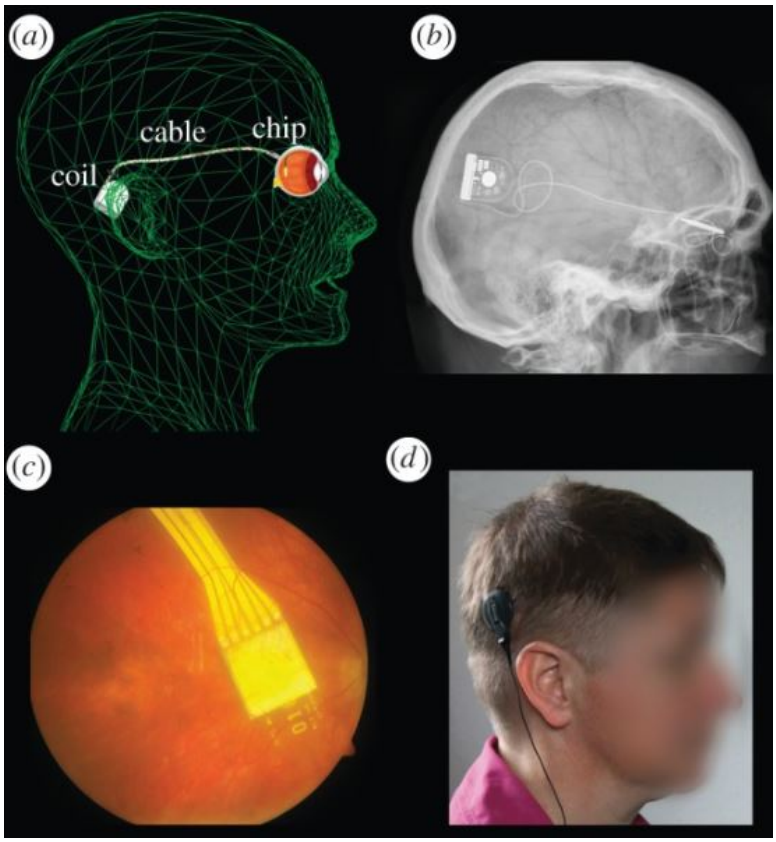

Figure 3.4: The Alpha IMS: (a) An image showing the basic schematic of the Alpha IMS where the coil near the ear provides power to the chip in the eye via a subdermal cable. (b) A brain scan of the implanted Alpha IMS showing the coil with a cable leading to the eye. (c) The chip placed beneath the fovea, where the center region of vision is focused and where cones are concentrated. (d) The primary external coil is kept magnetically above the subdermal coil behind the ear. Figure from Stingl et al. (2013a).

Suprachoroidal approaches have been pursued by Bionic Vision Australia (Ayton et al., 2014) and Osaka University in Japan (Fujikado et al., 2011).

Most recently, the photovoltaic subretinal prosthese PRIMA, was implanted in 5 patients with AMD, all of which could perceive visual patterns and did not decrease residual natural acuity (Palanker et al., 2020). Images captured by the camera are projected onto the retinal from glasses using near infared light (Figure 3.5). The projected light is

directly converted to electrical current from photovoltaic pixels. The prothesis contains 378 photovoltaic pixels each of which is 100 μm in diameter. The 3 patients with optimal placement of the implant demonstrated prosthetic acuity of 20/460 to 20/550, only 10 percent to 30 percent less than the sampling limit for the current pixel size (Palanker et al., 2020). Compared to the Argus II and Alpha IMS, the PRIMA surgical process is much simpler due to it's wireless nature. For their next step, they will test augmented reality glasses which will provide the prosthetic central vision alongside the natural peripheral vision for improved daily use (Palanker et al., 2020).

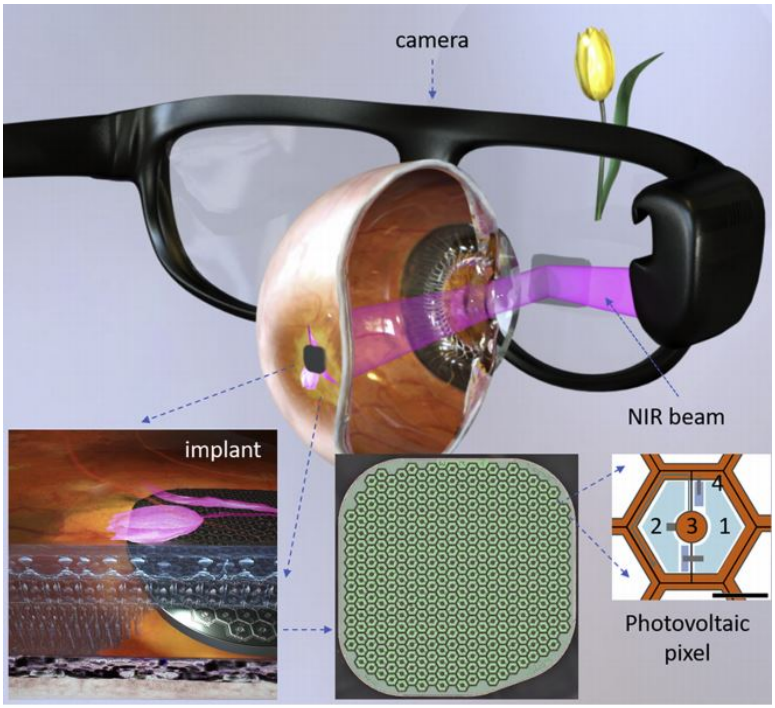

Figure 3.5: Photovoltaic PRIMA: Diagram showing the system for the photovoltaic subretinal implant PRIMA. It includes a camera integrated into augmented reality, with the processed imaged projected onto the retina using pulsed near-infared light. A subretinal wireless array converts the pulsed light into electrical current to stimulate adjacent inner retinal neurons. Every pixel has two diodes (1 and 2) with active (3) and return (4) electrodes. Figure from Palanker et al. (2020).

4

Discussion

Restoring spatial acuity is important for patients suffering from retinitis pigmentosa and AMD. Retinitis pigmentosa is considered rare and is estimated to affect 1 in 4000 people worldwide. Due to the profound blindness from retinitis pigmentosa, patients will benefit even from low to moderate visual acuity restoration. Therefore The Argus II and Alpha IMS, with visual acuities of 20/1260 and 20/2000 respectively, are better suited for patients with retinitis pigmentosa or other hereditary retinal degenerations. Due to the underperformance of the Argus II and Alpha IMS with respect to their sampling limits, one can conclude that pushing for smaller pixel sizes will not improve visual acuity above 20/200 and will be limited to patients with retinitis pigmentosa or other hereditary retinal degenerations.

AMD affects a much larger population than reinitis pigmentosa, around 8.7 percent of worlds population, or approximately 1 in 12 people. The number of people affected worldwide by AMD is projected to be 196 million by 2020 and rising to 288 million by 2040. Patients with AMD frequently retain some vision so devices with better visual acuity are

needed. PRIMA, the photovoltaic subretinal implant, had acuity in the range of 20/460 to 20/550 and is the best device to date for patients with AMD. PRIMA had only 10 to 30 percent less than the sampling limit for it's pixel size and thus with a smaller pixel size it may be possible to improve visual acuity over 20/200. A possible path forward for improvement in spatial resolution of retinal prosthesis is being pursued by Flores et al. (2019), with their novel 3-D honeycomb configuration that may restore functional center vision with acuity better than 20/100 (Flores et al., 2019).

Other methods of treatment for blinding disorders are being pursued, including lens regeneration using stem cells, transplantation of ganglion and photoreceptor cells in combination with bioengineering approaches (Stern et al., 2018).

Bibliography

Ayton, L. N., Blamey, P. J., Guymer, R. H., Luu, C. D., Nayagam, D. A. X., Sinclair, N. C., Shivdasani, M. N., Yeoh, J., McCombe, M. F., Briggs, R. J., Opie, N. L., Villalobos, J., Dimitrov, P. N., Varsamidis, M., Petoe, M. A., McCarthy, C. D., Walker, J. G., Barnes, N., Burkitt, A. N., Williams, C. E., Shepherd, R. K., Allen, P. J., & Bionic Vision Australia Research Consortium (2014). First-in-human trial of a novel suprachoroidal retinal prosthesis. *PloS One*, 9(12), e115239.

Boinagrov, D., Loudin, J., & Palanker, D. (2010). Strength–Duration Relationship for Extracellular Neural Stimulation: Numerical and Analytical Models. *Journal of Neurophysiology*, 104(4), 2236–2248.

Boinagrov, D., Pangratz-Fuehrer, S., Goetz, G., & Palanker, D. (2014). Selectivity of Direct and Network-mediated Stimulation of the Retinal Ganglion Cells with Epi-, Sub- and Intra-Retinal Electrodes. *Journal of neural engineering*, 11(2), 026008.

Brunel, N. & van Rossum, M. C. W. (2007). Quantitative investigations of electrical nerve excitation treated as polarization: Louis Lapicque 1907 · Translated by:. *Biological Cybernetics*, 97(5-6), 341–349.

Butterwick, A., Huie, P., Jones, B. W., Marc, R. E., Marmor, M., & Palanker, D. (2009).

Effect of shape and coating of a subretinal prosthesis on its integration with the retina. *Experimental Eye Research*, 88(1), 22–29.

Cooper, I. (2015). Doing physics with matlab biophysics hodgkin-huxley model: Membrane current.

da Cruz, L., Coley, B. F., Dorn, J., Merlini, F., Filley, E., Christopher, P., Chen, F. K., Wuyyuru, V., Sahel, J., Stanga, P., Humayun, M., Greenberg, R. J., Dagnelie, G., & Argus II Study Group (2013). The Argus II epiretinal prosthesis system allows letter and word reading and long-term function in patients with profound vision loss. *The British Journal of Ophthalmology*, 97(5), 632–636.

Eshraghi, A. A., Nazarian, R., Telischi, F. F., Rajguru, S. M., Truy, E., & Gupta, C. (2012). The cochlear implant: historical aspects and future prospects. *Anatomical Record (Hoboken, N.J.: 2007)*, 295(11), 1967–1980.

Flores, T., Huang, T., Bhuckory, M., Ho, E., Chen, Z., Dalal, R., Galambos, L., Kamins, T., Mathieson, K., & Palanker, D. (2019). Honeycomb-shaped electro-neural interface enables cellular-scale pixels in subretinal prosthesis. *Scientific Reports*, 9.

Freeman, D. K. & Fried, S. I. (2011). Multiple Components of Ganglion Cell Desensitization in Response to Prosthetic Stimulation. *Journal of neural engineering*, 8(1), 016008.

Fried, S. I., Lasker, A. C. W., Desai, N. J., Eddington, D. K., & Rizzo, J. F. (2009). Axonal sodium-channel bands shape the response to electric stimulation in retinal ganglion cells. *Journal of Neurophysiology*, 101(4), 1972–1987.

Fujikado, T., Kamei, M., Sakaguchi, H., Kanda, H., Morimoto, T., Ikuno, Y., Nishida,

K., Kishima, H., Maruo, T., Konoma, K., Ozawa, M., & Nishida, K. (2011). Testing of semichronically implanted retinal prosthesis by suprachoroidal-transretinal stimulation in patients with retinitis pigmentosa. *Investigative Ophthalmology & Visual Science*, 52(7), 4726–4733.

Galvani, L. (1791). Aloysii Galvani De viribus electricitatis in motu musculari commentarius.

Ghezzi, D., Antognazza, M. R., Maccarone, R., Bellani, S., Lanzarini, E., Martino, N., Mete, M., Pertile, G., Bisti, S., Lanzani, G., & Benfenati, F. (2013). A polymer optoelectronic interface restores light sensitivity in blind rat retinas. *Nature Photonics*, 7(5), 400–406.

Goetz, G. A. & Palanker, D. V. (2016). Electronic Approaches to Restoration of Sight. *Reports on progress in physics. Physical Society (Great Britain)*, 79(9), 096701.

Haim, M. (2002). Epidemiology of retinitis pigmentosa in Denmark. *Acta Ophthalmologica Scandinavica. Supplement*, (233), 1–34.

Ho, A. C., Humayun, M. S., Dorn, J. D., da Cruz, L., Dagnelie, G., Handa, J., Barale, P.-O., Sahel, J.-A., Stanga, P. E., Hafezi, F., Safran, A. B., Salzmann, J., Santos, A., Birch, D., Spencer, R., Cideciyan, A. V., de Juan, E., Duncan, J. L., Eliott, D., Fawzi, A., Olmos de Koo, L. C., Brown, G. C., Haller, J. A., Regillo, C. D., Del Priore, L. V., Arditi, A., Geruschat, D. R., Greenberg, R. J., & Argus II Study Group (2015). Long-Term Results from an Epiretinal Prosthesis to Restore Sight to the Blind. *Ophthalmology*, 122(8), 1547–1554.

Hodgkin, A. L. & Huxley, A. F. (1952). A quantitative description of membrane current

and its application to conduction and excitation in nerve. *The Journal of Physiology*, 117(4), 500–544.

Humayun, M., Propst, R., de Juan, E., McCormick, K., & Hickingbotham, D. (1994). Bipolar surface electrical stimulation of the vertebrate retina. *Archives of Ophthalmology (Chicago, Ill.: 1960)*, 112(1), 110–116.

Humayun, M. S., Dorn, J. D., da Cruz, L., Dagnelie, G., Sahel, J.-A., Stanga, P. E., Cideciyan, A. V., Duncan, J. L., Eliott, D., Filley, E., Ho, A. C., Santos, A., Safran, A. B., Arditi, A., Del Priore, L. V., Greenberg, R. J., & Argus II Study Group (2012). Interim results from the international trial of Second Sight's visual prosthesis. *Ophthalmology*, 119(4), 779–788.

Humayun, M. S., Prince, M., Juan, E. d., Barron, Y., Moskowitz, M., Klock, I. B., & Milam, A. H. (1999). Morphometric analysis of the extramacular retina from postmortem eyes with retinitis pigmentosa. *Investigative Ophthalmology & Visual Science*, 40(1), 143–148. Publisher: The Association for Research in Vision and Ophthalmology.

Liu, W., Vichienchom, K., Clements, M., DeMarco, S., Hughes, C., McGucken, E., Humayun, M., De Juan, E., Weiland, J., & Greenberg, R. (2000). A neuro-stimulus chip with telemetry unit for retinal prosthetic device. *IEEE Journal of Solid-State Circuits*, 35(10), 1487–1497. Conference Name: IEEE Journal of Solid-State Circuits.

London, M. & Segev, I. (2001). Synaptic scaling in vitro and in vivo. *Nature Neuroscience*, 4(9), 853–855.

Loudin, J. D., Simanovskii, D. M., Vijayraghavan, K., Sramek, C. K., Butterwick, A. F.,

Huie, P., McLean, G. Y., & Palanker, D. V. (2007). Optoelectronic retinal prosthesis: system design and performance. *Journal of Neural Engineering*, 4(1), S72–84.

Malmivuo, P., Malmivuo, J., & Plonsey, R. (1995). *Bioelectromagnetism: Principles and Applications of Bioelectric and Biomagnetic Fields*. Oxford University Press. Google-Books-ID: H9CFM0TqWwsC.

Marc, R. E. & Jones, B. W. (2003). Retinal remodeling in inherited photoreceptor degenerations. *Molecular Neurobiology*, 28(2), 139–147.

Marc, R. E., Jones, B. W., Watt, C. B., & Strettoi, E. (2003). Neural remodeling in retinal degeneration. *Progress in Retinal and Eye Research*, 22(5), 607–655.

Mathieson, K., Loudin, J., Goetz, G., Huie, P., Wang, L., Kamins, T. I., Galambos, L., Smith, R., Harris, J. S., Sher, A., & Palanker, D. (2012). Photovoltaic Retinal Prosthesis with High Pixel Density. *Nature Photonics*, 6(6), 391–397.

McCreery, D., Agnew, W., Yuen, T., & Bullara, L. (1990). Charge density and charge per phase as cofactors in neural injury induced by electrical stimulation. *IEEE Transactions on Biomedical Engineering*, 37(10), 996–1001. Conference Name: IEEE Transactions on Biomedical Engineering.

Morimoto, T., Kamei, M., Nishida, K., Sakaguchi, H., Kanda, H., Ikuno, Y., Kishima, H., Maruo, T., Konoma, K., Ozawa, M., Nishida, K., & Fujikado, T. (2011). Chronic implantation of newly developed suprachoroidal-transretinal stimulation prosthesis in dogs. *Investigative Ophthalmology & Visual Science*, 52(9), 6785–6792.

Palanker, D. & Goetz, G. (2018). Restoring Sight with Retinal Prostheses. *Physics today*, 71(7), 26–32.

Palanker, D., Le Mer, Y., Mohand-Said, S., Muqit, M., & Sahel, J. A. (2020). Photovoltaic Restoration of Central Vision in Atrophic Age-Related Macular Degeneration. *Ophthalmology*.

Purves, D., Augustine, G. J., Fitzpatrick, D., Katz, L. C., LaMantia, A.-S., McNamara, J. O., & Williams, S. M. (2001). Anatomy of the Eye. *Neuroscience. 2nd edition*. Publisher: Sinauer Associates.

Ratnayaka, J. A., Serpell, L. C., & Lotery, A. J. (2015). Dementia of the eye: the role of amyloid beta in retinal degeneration. *Eye*, 29(8), 1013–1026.

Sekirnjak, C., Hottowy, P., Sher, A., Dabrowski, W., Litke, A. M., & Chichilnisky, E. J. (2006). Electrical stimulation of mammalian retinal ganglion cells with multielectrode arrays. *Journal of Neurophysiology*, 95(6), 3311–3327.

Smith, W., Assink, J., Klein, R., Mitchell, P., Klaver, C. C., Klein, B. E., Hofman, A., Jensen, S., Wang, J. J., & de Jong, P. T. (2001). Risk factors for age-related macular degeneration: Pooled findings from three continents. *Ophthalmology*, 108(4), 697–704.

Sramek, C., Paulus, Y., Nomoto, H., Huie, P., Brown, J., & Palanker, D. (2009). Dynamics of retinal photocoagulation and rupture. *Journal of Biomedical Optics*, 14(3), 034007.

Stern, J. H., Tian, Y., Funderburgh, J., Pellegrini, G., Zhang, K., Goldberg, J. L., Ali, R. R., Young, M., Xie, Y., & Temple, S. (2018). Regenerating Eye Tissues to Preserve and Restore Vision. *Cell stem cell*, 22(6), 834–849.

Stingl, K., Bartz-Schmidt, K. U., Besch, D., Braun, A., Bruckmann, A., Gekeler, F., Greppmaier, U., Hipp, S., Hörtdörfer, G., Kernstock, C., Koitschev, A., Kusnyerik, A., Sachs, H., Schatz, A., Stingl, K. T., Peters, T., Wilhelm, B., & Zrenner, E. (2013a). Artificial vision with wirelessly powered subretinal electronic implant alpha-IMS. *Proceedings. Biological Sciences*, 280(1757), 20130077.

Stingl, K., Bartz-Schmidt, K. U., Besch, D., Chee, C. K., Cottriall, C. L., Gekeler, F., Groppe, M., Jackson, T. L., MacLaren, R. E., Koitschev, A., Kusnyerik, A., Neffendorf, J., Nemeth, J., Naeem, M. A. N., Peters, T., Ramsden, J. D., Sachs, H., Simpson, A., Singh, M. S., Wilhelm, B., Wong, D., & Zrenner, E. (2015). Subretinal Visual Implant Alpha IMS – Clinical trial interim report. *Vision Research*, 111, 149–160.

Stingl, K., Bartz-Schmidt, K.-U., Gekeler, F., Kusnyerik, A., Sachs, H., & Zrenner, E. (2013b). Functional Outcome in Subretinal Electronic Implants Depends on Foveal Eccentricity. *Investigative Ophthalmology & Visual Science*, 54(12), 7658–7665. Publisher: The Association for Research in Vision and Ophthalmology.

Stronks, H. C. & Dagnelie, G. (2014). The functional performance of the Argus II retinal prosthesis. *Expert review of medical devices*, 11(1), 23–30.

Suzuki, S., Humayun, M. S., Weiland, J. D., Chen, S.-J., Margalit, E., Piyathaisere, D. V., & de Juan, E. (2004). Comparison of electrical stimulation thresholds in normal and retinal degenerated mouse retina. *Japanese Journal of Ophthalmology*, 48(4), 345–349.

Tsai, D., Morley, J. W., Suaning, G. J., & Lovell, N. H. (2009). Direct activation and temporal response properties of rabbit retinal ganglion cells following subretinal stimulation. *Journal of Neurophysiology*, 102(5), 2982–2993.

Wandell, B., ell, & Login, S. U. |. T. o. U. |. (1995). *Foundations of Vision Chapter 3: The Photoreceptor Mosaic*. Library Catalog: foundationsofvision.stanford.edu.

Wang, G., Liu, W., Sivaprakasam, M., & Kendir, G. (2005). Design and analysis of an adaptive transcutaneous power telemetry for biomedical implants. *IEEE Transactions on Circuits and Systems I: Regular Papers*, 52(10), 2109–2117. Conference Name: IEEE Transactions on Circuits and Systems I: Regular Papers.

Weitz, A. C., Nanduri, D., Behrend, M. R., Gonzalez-Calle, A., Greenberg, R. J., Humayun, M. S., Chow, R. H., & Weiland, J. D. (2015). Improving the spatial resolution of epiretinal implants by increasing stimulus pulse duration. *Science translational medicine*, 7(318), 318ra203.

Wong, W. L., Su, X., Li, X., Cheung, C. M. G., Klein, R., Cheng, C.-Y., & Wong, T. Y. (2014). Global prevalence of age-related macular degeneration and disease burden projection for 2020 and 2040: a systematic review and meta-analysis. *The Lancet Global Health*, 2(2), e106–e116.

Zrenner, E., Bartz-Schmidt, K. U., Benav, H., Besch, D., Bruckmann, A., Gabel, V.-P., Gekeler, F., Greppmaier, U., Harscher, A., Kibbel, S., Koch, J., Kusnyerik, A., Peters, T., Stingl, K., Sachs, H., Stett, A., Szurman, P., Wilhelm, B., & Wilke, R. (2011). Subretinal electronic chips allow blind patients to read letters and combine them to words. *Proceedings of the Royal Society B: Biological Sciences*, 278(1711), 1489–1497. Publisher: Royal Society.